Prediction of Interaction of Citric Acid Modified Cellulose with Water Region Using Molecular Modelling Technique

Wan Nor Asyikin Wan Mohamed Daid, Nornizar Anuar

Faculty of Chemical Engineering, Universiti Teknologi Mara

Abstract— In this paper, chemically modified cellulose was used instead of cellulose as it offers higher adsorption capacities, great chemical strength and good resistance to heat. As part of Phyto-Adsorption Remediation Method, CAMC was used to treat ferric ion. However, there is a large possibility that CAMC molecule might interact with water molecule that contain hydrogen bond and hence pose as a competitor to ferric acid and reduces the efficiency of CAMC in ferric ion removal. Thus, the aim of this work is to identify the most stable hydrogen bond between CAMC and water, by using a computational technique. The interaction between the water molecules and CAMC was observed by varying the volume of water molecule with modified cellulose by an expansion in amorphous region. The simulation result showed that for water loading less than 20 molecules, the interaction between water molecules and CAMC is higher at temperature 311K, whilst for water loading higher than 20 molecules, the interaction weakens at higher temperature. This work proved that water molecules have the tendency to bind to hydroxyl group of glucose ring, to oxygen of ester and to oxygen of anhydride acid of the CAMC molecule. The calculation of coordination number has shown that the number of atoms present in the first hydration shell (of radius < 2.5Å) is more as the temperature increases from 298K to 311K. Whilst, at radius >2.5Å, cell temperature is not significant to the number of atoms present.

Keywords— Adsorption; non-bonded interaction; hydrogen bond; dynamics simulation.

I. INTRODUCTION

Cellulose is a polymer of β -D-glucose units linked together by glycosidic bonds to form cellobiose, and is a building block of the cellulose chain. Cellulose can form crystalline structure and stabilized by the dense hydrogen bonding (H-bond) network constructed among the crystalline-ordered polysaccharide chains (Shen & Gnanakaran, 2009). In recent years, the use of cellulose-based biodegradable material has become a very attractive selection in heavy metal removal in solution. Cellulose, one of the remarkable pure and naturally occurring organic polymer consists of units of anhydroglucose held together by β -(1,4)-glycosidic linkages in a giant straight chain molecule (Bian et. al, 2012; Demirbas, 2008). Raw material of cellulose can be from a variety of sources such as annual plants, microbes, animals and wood.

Plant based cellulose is known to be an excellent heavy metal and toxicity remover (Malik et al., 2016), however chemically modified cellulose has shown higher adsorption capacities for removal heavy metal toxicity than unmodified forms (Sanna et al., 2016). Pure cellulose has limited application and hence modification is favoured to produce substances that have different properties from cellulose, yet they are of renewable origin and biodegradable. An ester linkage or cellulose ester is produced when hydroxyl groups of cellulose is substituted by less polar ester group and this esterification has increased the carboxylic content of the cellulose as well as the sorption of divalent metal ions (Ramirez et. al, 2017; O'Connell et. al, 2008).

Cellulose can be modified using citric acid and forms citric acid modified cellulose (CAMC). Cellulose can be modified by the addition of the carbonyl groups (Firmansyah et al., 2017), and citric acid is known to be the most effective solvent as it has supply of carboxyl group that can used to increase the number of carboxyl group in the modified cellulose (Li et al., 2008). The presence of hydroxyl and carboxyl groups within the chemical structure of citric acid promote the availability of active sites for the adsorption of ions, which is proven in the adsorption capacity of both yam peels and palm bagasse by 20 and 10%, respectively; when treated with modified citric acid (Tejada et. al, 2016). An increment of carboxyl group and total negative charge contributed by citric acid on to the soybean hulls has successfully removed Zn (II) from aqueous solution (Yadav et. al, 2017). Modification of cellulose using citric acid involves two major steps; i.e. (i) the formation of reactive internal anhydride (5 member ring formation) between two adjacent carboxylic groups of the citric acid molecule, resulting the loss of one molecule of water, and (ii) the anhydride reaction with hydroxyl group to form an ester linkage between the two substrates. In the later step, two acid groups remain on the citric acid molecule (James et al., 2006), and this modified cellulose is more effective for heavy metal removal, when applied after base extraction to enhance cation exchange capacity. Molecule of cellulose has higher potentially to bind with metal cations and CAMC improves the metal ion absorption chemically (James et al., 2006) and better heavy metal absorption capability due to its thermoplastic behaviour (Raj et al., 1992). At the same time carboxyl groups are polar and soluble in water (Morrison, 1992).

In this work, the interactions between CAMC and water molecules were assessed using a molecular modelling technique. This was carried out with the intention to determine their specific interactions and the adsorption competition they might pose when heavy metals are present in the solution. The interaction effect was examined between varied numbers of water molecules and a single CAMC molecule, and the effect of temperature on the interaction between them by using a molecular modelling technique.

Theoretical Background. Radial distribution function or sometimes referred to as pair correlation function, gives a measure of the probability of atoms present in a spherical shell with a distance, r from a central atom (reference atom). Figure 1 shows the radial distribution function of particles in a basic atomic liquid.

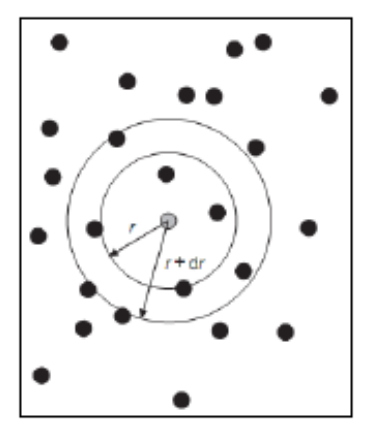


Fig. 1: Radial distribution function in the atom position in the cell from a random reference atom.

The number of particle surrounding a central atom or coordination number can be determined by integrating radial distribution function (Egami et al., 2013).

$$RDF = 4\pi r^2 \rho g_i(r) \tag{1}$$

Integration of Equation (1) gives the Equations as follows;

$$n = \int_{r_1}^{r_2} 4\pi r^2 \rho g_i(r) dr$$

$$n = \frac{4}{3} \pi \rho [(r^3 g_2(r^2) - (r^3 g_1(r^1))]$$
(2)

where r^1 and r^2 are radius and g_i (r) is the peak of RDF equivalent to the coordination shell while ρ is the density of the complex structure.

II. METHODOLOGY

A. Material and Computational Method

Material. Figure 2 shows the structure of a trisaccharide molecule and the citric acid modified cellulose (CAMC). Glucose is a building block of cellulose, and the trsaccharide consists of three glucose molecules (C₆H₁₂) with 48 atoms, whilst CAMC molecule consists of 161 atoms. The CAMC is an ester cellulose produced by an esterification of cellulose with citric acid at high temperature. The cellulosic hydroxyl groups combine with citric acid anhydride form an ester linkage and introduce carboxyl groups through crosslinking reaction, which stabilize the modified cellulose. The presence free carboxyl groups increases its ability for metal ion adsorption (Nguyen et al., 2013), and any hydroxyl-containing substances especially water molecules.

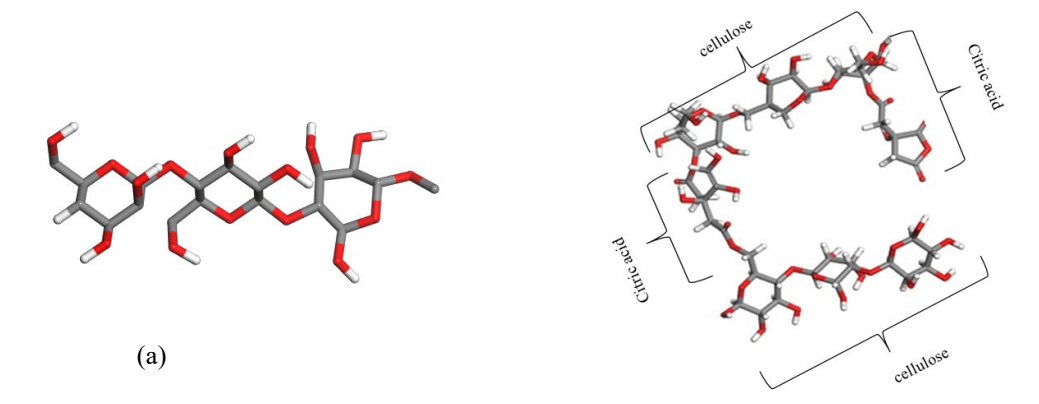


Fig. 2: Schematics of (a) trisaccharide molecule, a building block of cellulose, and (b) a modified cellulose chain (CAMC) (Nguyen et al., 2013). A cellulose can consists of n number or glucose.

Computational Technique. In this study, Materials Studio (MS) 7.0 from Accelrys was used as a molecular modelling simulation tool to measure an interaction between CAMC and the water molecules. The calculation of interaction energy, geometry optimizations, and dynamics simulation were performed using Dreiding force field. Dynamic simulation was carried out using the amorphous cell module,

which is an embedded module in MS. The analysis of the molecular modelling simulation was determined by radial distribution function (RDF), and coordination number of the atoms, associated to RDF.

Creation of 3D periodic structures of CAMC and water molecule. The CAMC and water molecules were first drawn using embedded tools available in the MS. The molecules were subjected to energy minimization and geometry optimization procedures, using a built up module in MS. A periodic amorphous cell model containing CAMC and water molecules was built with specific lattice dimensions, depending on the number of molecules (loading) and the size of the molecules present in the cell. Table 1 shows the lattice dimensions (hence the cell volume) correspond to the number of loading of water molecules in the system. In this study, the CAMC molecule was kept to be at one, whilst the numbers of water molecules were varied. The density of the cell was set as 1 g/cc, and the output of the simulation was set as 50 frames. Two different temperatures were used; 298K and 311K representing the possible water temperature and was set during the construction of the amorphous cell of CAMC-H₂O and dynamic simulation of the system.

Table 1: Parameters adopted in this study, in which the cubic cell composition of one CAMC chain and varying number of water molecules, with its

respective cell lattice parameters and cell volume.

Molecules	Loading	Weight (%)	Cubic lattice cell parameters, a (Å) = b (Å) = c (Å)	Cell volume (A°³)
CAMC	1	98.6	13.0	2197
Water	1	1.4		
CAMC	1	64.4	15.0	3363.5
Water	40	35.6		
CAMC	1	47.5	16.6	4560.3
Water	80	52.5		
CAMC	1	37.6	18.0	5756.5
Water	120	62.4		
CAMC	1	31.2	19.1	6953.7
Water	160	68.8		
CAMC	1	26.6	20.1	8149.7
Water	200	73.4		
CAMC	1	23.2	21.1	9347.3
Water	240	76.8		

Geometry Optimization of the Periodic System. The periodic cell built, which contain CAMC and water molecules were subjected to geometry optimization, in search for stable geometry before dynamic simulation can be carried out. During this process, the charges of the atoms responded in such a way either by moving away from the same charges or closer to the opposing charges (Johnson et al., 2006). At this point, the coordinates of the atoms were adjusted, and hence the energy of the structures produced to a stationary point, and results in zero for overall atomic forces. The force field used for this study to calculate the total energy of the system was Dreiding, with Ewald method as the energy summation method for the non-bonded interactions. The atomic charges were calculated using Gasteiger.

Molecular Dynamics Run for the Periodic Systems. The dynamic simulation was carried out after geometry optimization to identify the potential functional groups attached to the water molecule during interaction. In dynamic system, the cell pressure was fixed at 1 atm $(1 \times 10^{-4} \text{GPA})$ for temperature at 298K and 311K. The type of ensemble used for each different water molecules loading was NPT (constant pressure-constant temperature), whilst the thermostat and barostat setting were set as Berendsen. The total simulation time of 25ps with the numbers of steps was set at 25000, and with frame output for every 500 steps. Ewald was also used as the non-bonded energy summation method, with Gasteiger method for atomic charges calculation.

III. RESULTS AND DISCUSSION

The interactions of CAMC with varying loadings of water molecule were determined at two different temperatures which was at 298K (25°C) and 311K (38°C). Figure 3 shows the intermolecular interaction between CAMC and total water loading, measured as a radial distribution function (RDF), at two different cell temperatures, representing the CAMC and water environment conditions. From figure 3(a), the first peak shown by 1CAMC-1H₂O system is at 2.11Å for temperature of 298K, whilst as the temperature of the cell was increased to 311K, the first peak shifted to 2.03Å. However, for the system containing 1CAMC-120H₂O, the first peak occurs at 1.61Å for the system at temperature 298K, and the first H-bond interaction recorded for this system is at 1.85Å. The shorter radius shown by the results indicate that the hydrogen bonds formed are stronger that the first peak shown at higher radius distance. For 1CAMC-1H2O system, the shift of peak to a shorter radius indicates that the hydrogen binding is higher as temperature of the solution increases. It is postulated that the adsorption capacity of CAMC increases with temperature (Chao-Yin et al. (2014)), in which it was suggested that the affinity of binding sites for water molecule increases with temperature as adsorption of water molecule onto CAMC was endothermic. Hydrogen bond can exists at a distance less than 3.25 Å between any two oxygen atoms and the OH vector angle from the same molecules was less than 35° (Raghavan et al., 1991).

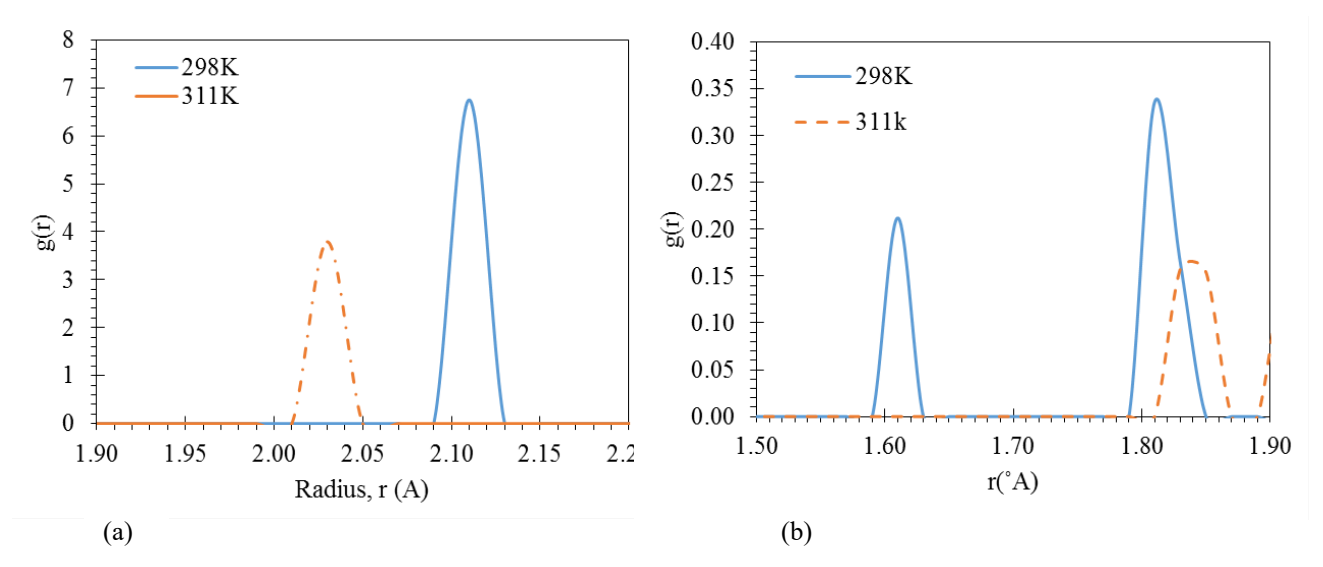


Fig. 3: Radial distribution function of interaction between (a) 1CAMC and 1H₂O, and (b) 1CAMC and 120 H₂O at 298K and 311K.

However, the result shown in Figure 3(b) does not support the finding by Chao-Yin et al. (2014) in which it was recorded that as temperature increases, the hydrogen bond was detected at bigger radius than system with lower temperature. Figure 4 shows the variation of water loading with radius creating hydrogen bond, extracted from the RDF analysis. The points were fitted using a power equation. The result shows that for water loading less than 20 molecules, at temperature 311K, the interaction of water and CAMC are closer compared to at temperature of 298K. Nevertheless, as the water loading increases, it is apparent that the measured radius is shorter at lower temperature, hence indicates that the hydrogen bond adsorption is better at lower temperature. Figure 5 shows the radial distribution function of interaction between self-molecules, i.e. water and water; and within the CAMC molecules. The result shows that the first peaks recorded for both CAMC and water molecules almost overlap (within the range of 0.95 – 0.99Å) one another, regardless of the temperature of the system.

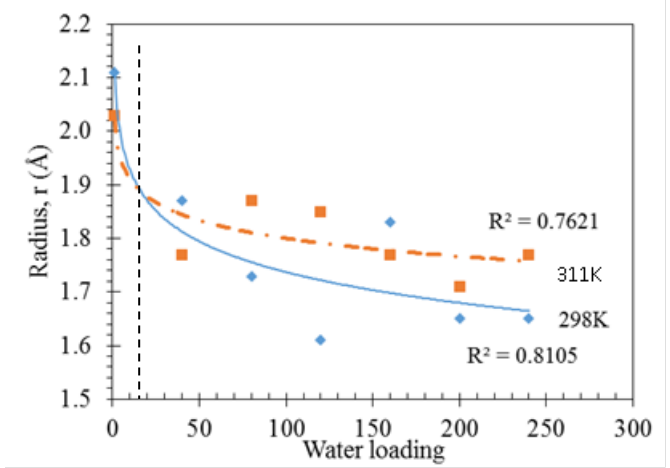


Fig. 4: The effect of CAMC-H₂O interactions at various water loading and temperature.

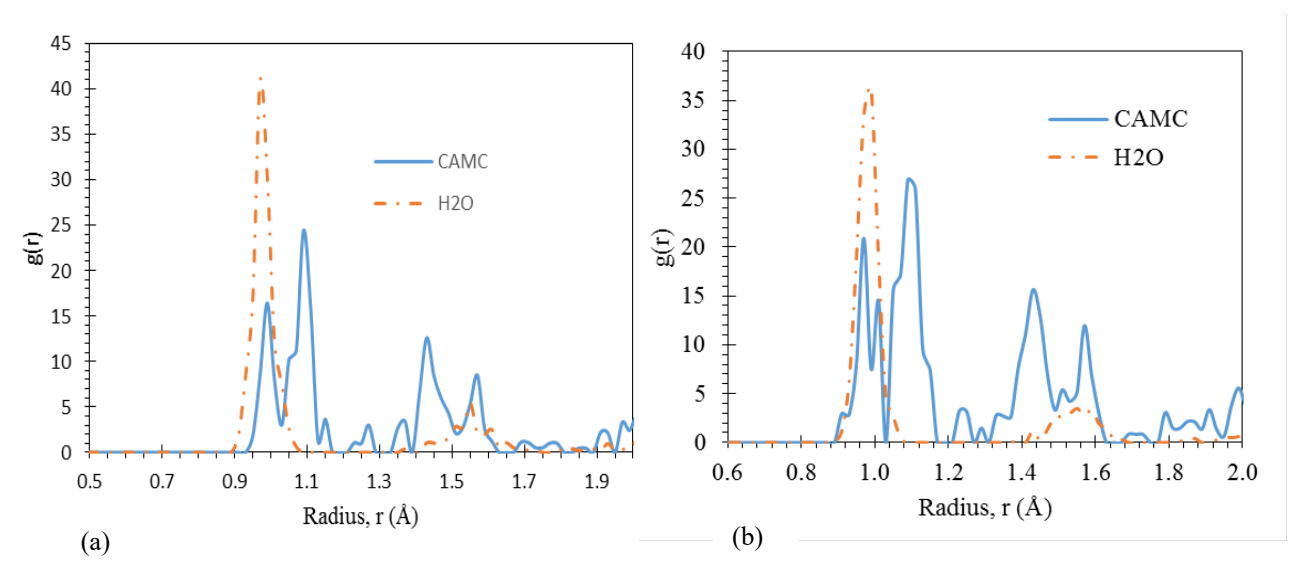


Fig. 5: Radial distribution function of interaction between (a) 1CAMC and 80H₂O at 311K, and (b) 1CAMC and 120H₂O at 298K.

CAMC-H₂O hydrogen bond. As shown in Figure 6, hydrogen bond (dashed line) is formed between a water molecule and functional groups of CAMC structure. Figure 6(a) shows that the hydrogen from the water molecule binds to the hydroxyl group of the glucose ring. On the other hand, for the cell with 40H₂O and 1 CAMC, the hydrogen bond was observed formed between hydrogen atom of water and the oxygen atom of ester group from citric acid molecule (denoted by (I) in Figure 6(b)). Meanwhile, another hydrogen bond observed is between hydrogen atom of water with oxygen atom of two glucose (O-H) ring from CAMC molecule (denoted as (II) in Figure 6(b)). This shows that the water molecules adsorbed to hydroxyl group could pose as a competition to the adsorption of ions (in the case of metal ion in water) to the CAMC, as the binding of hydrogen of water molecules to oxygen of ester and to oxygen of anhydride acid of the CAMC molecule might not affect metal ion from water. This results support the postulation that modification of CAMC prepares more adsorption sites (Nguyen et al., 2013). Hydrogen bond formed when a hydrogen atom bound to an electronegativity atom such as nitrogen, fluorine of oxygen and transferred its charge to nearby attracted electronegative atom (Brini et al., 2017). Angles and lengths of hydrogen bond will change based on polarization shifts in different environments of hydrogen-bonded and when water molecules bound to solutes and ion. The strength of the hydrogen bond varies linearly on its distance. Hence the shorter the distance of hydrogen bond formed, the stronger the hydrogen bonding (Chaplin, 2007).

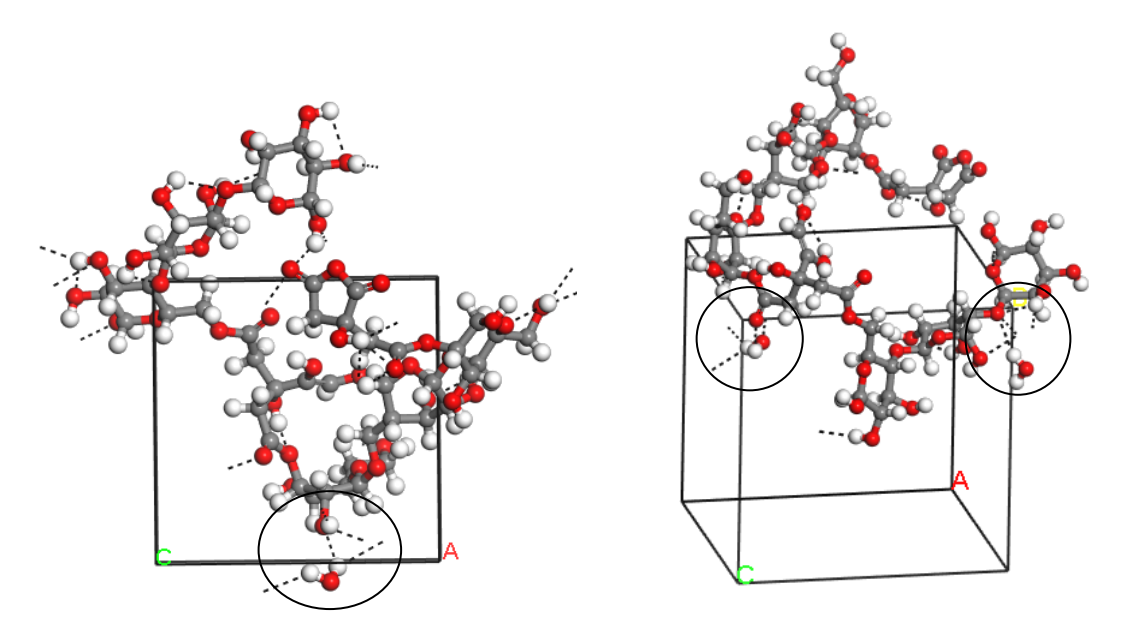


Fig. 6: Interaction of H₂O molecule with the OH of the cellulose ring, observed in the periodic cell containing (a) 1H₂O molecule and 1CAMC molecule, and (b) 40H₂O and 1CAMC molecule, at their lowest energy and at the most stable geometry configuration. The remaining of H₂O molecules, which not participate in the binding at this point we deleted for clarity purposes.

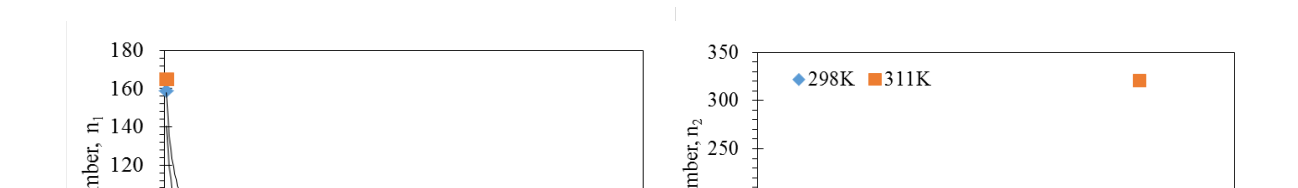


Fig. 7: Coordination number within the hydration shell, calculated from RDF analysis.

Figure 7 shows the coordination number, n₁ contained in the hydration shell, and this data was extracted from the RDF analysis. The coordination numbers were calculated at two coordination shell, which were first hydration shell (~1.5-2.5 Å) and second hydration shell (~2.5-3.5 Å). The result shows in Figure 7(a) indicates that the number of atoms present in the first hydration shell increases as the temperature increases from 298K to 311K. Nevertheless, the number of atoms present in the first hydration shell is lesser as the water loading increases. However, the result shows in Figure 7(b) depicted that the number of atoms present in the second hydration shell is independent of temperature and water loading in the cell. The RDF result shows the possible interaction of hydrogen-bonding occurred between CAMC and loading of water molecule. However, the interaction between molecules of CAMC itself might occur in solution (William et al., 2012). This indicates that the first shell highest coordination number is contributed from the one CAMC and one H2O loading at 311K that involved 164.934 molecules show hydrogen bonding between their hydroxyl groups. The loading of one CAMC and 160 H2O (298K) at second shell revealed the highest coordination number which was 200.9779 molecules involved in the effective hydrogen-bonding interaction. In fact, the highest number of coordination number at a shorter distance verifying the good affinity between CAMC and water molecules.

IV. CONCLUSION

In this work, the following can be concluded:

- (1) The simulation result showed that for water loading less than 20 molecules, the interaction between water molecules and CAMC is higher at temperature 311K, whilst for water loading higher than 20 molecules, the interaction weakens at higher temperature.
- (2) The hydrogen of the water molecules have the tendency to bind to hydroxyl group of glucose ring, to oxygen of ester and to oxygen of anhydride acid of the CAMC molecule.
- (3) The number of atoms present in the first hydration shell (of radius < 2.5Å) is more as the temperature increases from 298K to 311K. Whilst, at radius >2.5Å, cell temperature is not significant to the number of atoms present.

ACKNOWLEDGMENT

The authors would like to express their gratitude to the Ministry of Higher Education, Malaysia for funding this work which was carried out at Universiti Teknologi MARA. This work is part of research grant 600-IRMI/MYRA5/3BESTARI (023/2017)

References

- [1] T. Shen & S.Gnanakaran, (2009). The Stability of Cellulose: A Perspective from the Statistical Mechanics of Hydrogen Bond Networks. Biophys. J., 96(April), 100–101.
- [2] J. Bian, X. P. Peng, P. Peng, F. Xu & R. S. Sun, (2012). Cellulose From Sugarcane Bagasse: Structural. BioResources, 7(4), 4626–4639.
- [3] A. Demirbas,(2008). Heavy metal adsorption onto agro-based waste materials: A review. Journal of Hazardous Materials, 157(2–3), 220–229. http://doi.org/10.1016/j.jhazmat.2008.01.024
- [4] R. Saravanan & L. Ravikumar, (2015). The Use of New Chemically Modified Cellulose for Heavy Metal Ion Adsorption and Antimicrobial Activities. Journal of Water Resource and Protection, 7(April), 530–545. http://doi.org/10.4236/jwarp.2015.76042
- [5] V. K. Varshney & S. Naithani, (2011). Cellulose Fibers: Bio- and Nano-Polymer Composites, 43–61. http://doi.org/10.1007/978-3-642-17370-7
- [6] A. C, Khazraji & S. Robert, (2013). Self-Assembly and Intermolecular Forces When Cellulose and Water Interact Using Molecular Modelling. Journal of Nanomaterials, 12.
- [7] D. S. Malik, C. K. Jain, & A. K. Yadav (2016). Removal of heavy metals from emerging cellulosic low-cost adsorbents: A review, 24
- [8] H. Sanna, B. Amit, & S. Mika, (2016). A review on modification methods to cellulose-based adsorbents to improve adsorption capacity. Science Direct. 18
- [9] J. A. Avila Ramirez, E. Fortunati, J. M. Kenny, L. Torre, & M. L. Foresti, (2017). Simple citric acid-catalyzed surface esterification of cellulose nanocrystals. Carbohydrate Polymers, 157, 1358–1364. http://doi.org/10.1016/j.carbpol.2016.11.008
- [10] D.W. O' Connell, C. Birkinshaw, & T. F. O' Dwyer, (2008). Heavy metal adsorbents prepared from the modification of cellulose: A review. Bioresource Technology, 99(15), 6709–6724. http://doi.org/10.1016/j.biortech.2008.01.036
- [11] D. M. James, M. R. Roger & S. Hong min, (2006). Effect of Citric Acid Modification of Aspen Wood on Sorption of Copper Ion. Journal of Natural Fibers, 16.

- [12] R. G. Raj, & B. V. Kokta, (1992). Mechanical Properties of Surface-Modified Cellulose Fiber-Thermoplastic Composites. Material and Chemicals from Biomass, 12.
- [13] C. Tejada, A. Herrera, & E. Ruiz (2016). Kinetic and isotherms of biosorption of Hg (II) using citric acid treated residual materials Cinética e isotermas de bioadsorción de Hg (II) usando materiales residuales tratados con ácido cítrico. Ingenieria Y Competividad, 18(1), 117–127.
- [14] J.S. Yadav, M. Soni & A. Lashkari, (2017). Equilibrium and Kinetic Studies of Zinc (II) Ion Adsorption from Aqueous Solution by Modified Soybean Hulls. International Referred Journal of Engineering and Science, 6(1), 30-35.
- [15] R. T. Morrison; R. N. Boyd (1992). Organic Chemistry (6th ed.). ISBN 0-13-643669-2
- [16] D. Firmansyah, B. Rumhayati, & Masruri, (2017). Modification of Pineapple Leaf Cellulose with Citric Acid for Fe2+ Adsorption. International Journal of ChemTech Research, 10, 7.
- [17] X. Li, Y. Tang, X. Cao, D. Lu, F. Luo, & W. Shao, (2008). Preparation and Evaluation of orange peel cellulose adsorbents for effective removal of cadmium, zinc, cobalt and nickel. Science Direct, 317(1-3), 512-521.
- [18] T. A. H. Nguyen, H. H. Ngo, W. S. Guo, J. Zhang, S. Liang, Q. Y. Yue, Q. Li, & T. V. Nguyen, (2013). Applicability of agricultural waste and by-products for adsorptive removal of heavy metals from wastewater. Science Direct, 12.
- [19] Accelrys Software Inc., Material Studio Modelling Environment, (2011). Accelrys Software Inc., San Diego, Calif, USA.
- [20] K. J. Johnson, R. T. Cygan, & J. B. Fein, (2006). Molecular simulations of metal adsorption to bacterial surfaces. Science Direct, 5076-5088.
- [21] [21] E. Brini, C. J. Fennell, M. Fernandez-Serra, B. Hribar-Lee, M. Luksic, & K. A. Dill, (2017). How Water's Properties are Encoded in Its Molecular Structure and Energies. Chemical Review, 117, 12385-12414.
- [22] M. Chaplin, (2007). Water's Hydrogen Bond Strength. 20.
- [23] K. Raghavan, M. R. Reddy, & M. L. Berkowitz, (1991). A Molecular Dynamics Study of the Structure and Dynamics of Water between Dilauroylphosphatidylethanolamine Bilayers. Langmuir 1992, 8.
- [24] Y. Delavoux, M. Gilmore, M. P. Atkins, M. Swadzba-Kwasny, & J. D. Holbrey, (2017). Intermolecular structure and hydrogen-bonding in liquid 1,2-propylene carbonate and 1,2-glycerol carbonate dettermined from neutron scattering. Physical Chemistry Chemical Physics (PCCP), 19, 2867-2876.
- [25] K. Chao-Yin, W. Chung-Hsin, & C. Meng-Jia, (2014). Adsorption of lead ions from aqueous solutions by citric acid-modified celluloses. Desalination and Water Treatment, 1-7.
- [26] T. Egami, & S. J. L. Billinge. (2013). Underneath the Bragg Peaks: Structural Analysis of Complex Materials. Elsevier Science.
- [27] B. O. D. William, C. B. David, & E. M. Sylvia, (2012). Structural Evidence for Inter-Residue Hydrogen Bonding Observed for Cellobiose in Aqueous Solution. Research gate, 11.
- [28] [28] C. Riccardo, & M. N. D. S. Cordeiro, (2016). Molecular Dynamics Simulation Study of the Selectivity of a Silica Polymer for Ibuprofen. Molecular Science. 17.